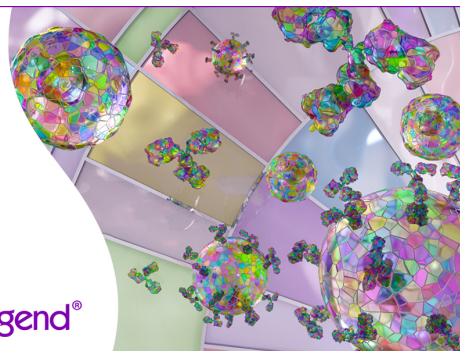


## Discover 25+ Color Optimized Flow Cytometry Panels

- Human General Phenotyping Panel
- Human T Cell Differentiation and Exhaustion Panel
- Human T Cell Differentiation and CCRs Panel

Learn more ▶

BioLegend®



## The Journal of Immunology

RESEARCH ARTICLE | AUGUST 01 2008

### IFN Regulatory Factor-1 Negatively Regulates CD4<sup>+</sup>CD25<sup>+</sup> Regulatory T Cell Differentiation by Repressing Foxp3 Expression<sup>1</sup> ✓

Alessandra Fragale; ... et. al

*J Immunol* (2008) 181 (3): 1673–1682.

<https://doi.org/10.4049/jimmunol.181.3.1673>

#### Related Content

Oncostatin M suppress activation of IL-17/Th17 via SOCS3 regulation in CD4<sup>+</sup> T cells of autoimmune arthritis (123.22)

*J Immunol* (May,2012)

Signs of Dendritic Cell Activation in the Lungs of Mice Exposed to Aerosols of Flavored Vaping Liquid

*J Immunol* (May,2023)

# IFN Regulatory Factor-1 Negatively Regulates CD4<sup>+</sup>CD25<sup>+</sup> Regulatory T Cell Differentiation by Repressing Foxp3 Expression<sup>1</sup>

Alessandra Fragale,\* Lucia Gabriele,<sup>†</sup> Emilia Stellacci,\* Paola Borghi,<sup>†</sup> Edvige Perrotti,\* Ramona Ilari,\* Angela Lanciotti,\* Anna Lisa Remoli,\* Massimo Venditti,<sup>†</sup> Filippo Belardelli,<sup>†</sup> and Angela Battistini<sup>2\*</sup>

Regulatory T (Treg) cells are critical in inducing and maintaining tolerance. Despite progress in understanding the basis of immune tolerance, mechanisms and molecules involved in the generation of Treg cells remain poorly understood. IFN regulatory factor (IRF)-1 is a pleiotropic transcription factor implicated in the regulation of various immune processes. In this study, we report that IRF-1 negatively regulates CD4<sup>+</sup>CD25<sup>+</sup> Treg cell development and function by specifically repressing Foxp3 expression. IRF-1-deficient (IRF-1<sup>-/-</sup>) mice showed a selective and marked increase of highly activated and differentiated CD4<sup>+</sup>CD25<sup>+</sup>Foxp3<sup>+</sup> Treg cells in thymus and in all peripheral lymphoid organs. Furthermore, IRF-1<sup>-/-</sup> CD4<sup>+</sup>CD25<sup>-</sup> T cells showed extremely high bent to differentiate into CD4<sup>+</sup>CD25<sup>+</sup>Foxp3<sup>+</sup> Treg cells, whereas restoring IRF-1 expression in IRF-1<sup>-/-</sup> CD4<sup>+</sup>CD25<sup>-</sup> T cells impaired their differentiation into CD25<sup>+</sup>Foxp3<sup>+</sup> cells. Functionally, both isolated and TGF- $\beta$ -induced CD4<sup>+</sup>CD25<sup>+</sup> Treg cells from IRF-1<sup>-/-</sup> mice exhibited more increased suppressive activity than wild-type Treg cells. Such phenotype and functional characteristics were explained at a mechanistic level by the finding that IRF-1 binds a highly conserved IRF consensus element sequence (IRF-E) in the *foxp3* gene promoter in vivo and negatively regulates its transcriptional activity. We conclude that IRF-1 is a key negative regulator of CD4<sup>+</sup>CD25<sup>+</sup> Treg cells through direct repression of Foxp3 expression. *The Journal of Immunology*, 2008, 181: 1673–1682.

Tolerance is critical for prevention of autoimmunity and maintenance of immune homeostasis by active suppression of inappropriate immune responses. Suppression has a dedicated population of T cells that control the responses of other T cells. This cell population, referred to as regulatory T (Treg)<sup>3</sup> cells, actually comprises several subsets, including naturally occurring CD4<sup>+</sup>CD25<sup>+</sup> Treg cells that arise in thymus. Once generated, thymic Treg cells are exported to peripheral tissues, and comprise 5–10% of peripheral CD4<sup>+</sup> T cells (1–3). CD4<sup>+</sup>CD25<sup>+</sup> Treg cells are characterized by constitutive expression of IL-2R $\alpha$  (CD25), CTLA-4, and glucocorticoid-induced TNFR family-related gene; moreover, they express CD62L ligand (CD62L) and are mainly CD45RB<sup>low</sup> (4). In contrast to cell surface markers, which can be shared with other T cells populations, the forkhead/winged-helix family transcriptional repressor Foxp3 is specifically expressed in CD4<sup>+</sup>CD25<sup>+</sup> Treg cells and rigorously controls their

development and function (5–7). Functionally after TCR stimulation, CD4<sup>+</sup>CD25<sup>+</sup> Treg cells can mediate strong suppression of proliferation and IL-2 production by CD4<sup>+</sup> T cells both in vivo and in vitro (8). Although mechanisms of suppression are not fully understood, they appear to be cell contact-mediated, whereas the relative contribution of soluble cytokines remains controversial with differences between in vitro and in vivo results (1, 8, 9). Indeed, the involvement of cytokines in the suppressor function of CD4<sup>+</sup>CD25<sup>+</sup> Treg cells has been proposed in vivo, where they are able to produce IL-10 and TGF- $\beta$  (10–12), and importantly, IL-10 activity has been recently associated with the function of TGF- $\beta$ -induced CD4<sup>+</sup>CD25<sup>-</sup>CD45RB<sup>low</sup> cells (13).

Beside naturally occurring CD4<sup>+</sup>CD25<sup>+</sup> Treg cells, CD4<sup>+</sup>CD25<sup>+</sup> Treg cells can also be induced (iTreg) in vivo or in vitro after TCR stimulation and TGF- $\beta$  treatment, acquiring expression of CD25 and Foxp3 both in mice (14–16) and humans (17–20), although with characteristic functional differences (20). Despite extensive studies on the role of Foxp3 in inducing and maintaining tolerance, little information on regulation of its expression is available.

Transcription factors of the IFN regulatory factor (IRF) family participate in the early host response to pathogens, in immunomodulation and hematopoietic differentiation (21). Nine members of this family have been identified based on a unique helix-turn-helix DNA binding domain, located at the N terminus that is responsible for binding to the IRF consensus element (IRF-E) (21). The first member of the family, IRF-1, was originally identified as a protein that binds the *cis*-acting DNA elements in the *ifn $\beta$*  gene promoter and the IRF-E (also referred to as the IFN-stimulated response element; ISRE), in the promoters of IFN- $\alpha\beta$ -stimulated genes (22). IRF-1 is expressed at low basal levels in all cell types examined, but accumulates in response to several stimuli

\*Department of Infectious, Parasitic and Immunomediated Diseases, and <sup>†</sup>Department of Cell Biology and Neurosciences, Istituto Superiore di Sanità, Rome, Italy

Received for publication October 31, 2007. Accepted for publication May 16, 2008.

The costs of publication of this article were defrayed in part by the payment of page charges. This article must therefore be hereby marked *advertisement* in accordance with 18 U.S.C. Section 1734 solely to indicate this fact.

<sup>1</sup> This work was supported in part by grants from the Italian AIDS Project, the Italian Ministry of Health, the Istituto Superiore di Sanità-National Institutes of Health Scientific Cooperation agreement and ISS-ACC program 3 (to A.B. and F.B.).

<sup>2</sup> Address correspondence and reprint requests to Dr. Angela Battistini, Department of Infectious, Parasitic and Immunomediated Diseases, Istituto Superiore di Sanità, viale Regina Elena 299, 00161 Rome, Italy. E-mail address: battistini@iss.it

<sup>3</sup> Abbreviations used in this paper: Treg, regulatory T; iTreg, induced Treg; IRF, IFN regulatory factor; IRF-E, IRF consensus element; DC, dendritic cell; CD62L, CD62 ligand; ChIP, chromatin immunoprecipitation; KO, knockout; WT, wild type.

Copyright © 2008 by The American Association of Immunologists, Inc. 0022-1767/08/\$2.00

and cytokines including IFN- $\gamma$ , the strongest IRF-1 inducer (22). Intensive functional analyses conducted on this transcription factor have revealed a remarkable functional diversity in the regulation of cellular responses through the modulation of different sets of genes, depending on cell type, state of the cell, and/or nature of the stimuli (21).

We and others have shown that IRF-1 affects the differentiation of both lymphoid and myeloid lineages (22–28). In particular, studies in knockout (KO) mice have implicated IRF-1 in the regulation of various immune processes: impairment of CD8<sup>+</sup> T cell and NK cell maturation, impaired IL-12 macrophage production, exclusive Th2 differentiation, and defective Th1 responses have all been observed (22–26). As a result, IRF-1<sup>-/-</sup> mice are highly susceptible to infections, for which effective host control is associated with a Th1 immune response (24). In contrast, these mice are characterized by increased resistance to several autoimmune diseases such as collagen-induced arthritis, experimental autoimmune encephalomyelitis, *Helicobacter pylori*-induced gastritis, induced lymphocytic thyroiditis, insulinitis, or diabetes (29–32).

Recently, we reported that IRF-1<sup>-/-</sup> mice display a prevalence of dendritic cell (DC) subsets with immature and tolerogenic features that were unable to undergo full maturation after stimulation. Moreover, IRF-1<sup>-/-</sup> DC conferred increased suppressive activity to CD4<sup>+</sup>CD25<sup>+</sup> Treg cells (33). Because there is growing evidence that immature or partially matured DC can induce tolerance (34, 35), we hypothesized that IRF-1 could play a role in Treg development and function. In this study, we analyzed the CD4<sup>+</sup>CD25<sup>+</sup> compartment in IRF-1<sup>-/-</sup> mice and we found that in vivo IRF-1 deficiency resulted in a selective and marked increase in highly differentiated and activated CD4<sup>+</sup>CD25<sup>+</sup>Foxp3<sup>+</sup> Treg cells, whereas reintroduction of IRF-1 by retrovirus transduction impaired TGF- $\beta$ -mediated differentiation of IRF-1<sup>-/-</sup> CD4<sup>+</sup>CD25<sup>-</sup> T cells into CD4<sup>+</sup>CD25<sup>+</sup>Foxp3<sup>+</sup> Treg cells. At molecular level, we show that IRF-1 plays a direct role in the generation and expansion of CD4<sup>+</sup>CD25<sup>+</sup> Treg cells specifically repressing Foxp3 transcriptional activity. Our results, therefore, highlight a unique role for IRF-1 as regulator of Foxp3, thus pointing to IRF-1 as a specific tool to control altered tolerance.

## Materials and Methods

### Mice

IRF-1<sup>-/-</sup> mice (23) (The Jackson Laboratory) were provided by Dr. Y. Tagaya (National Cancer Institute, National Institutes of Health, Bethesda, MD). The B6.129-IRF1<sup>-/-</sup> mice, which are on a hybrid C57BL/6  $\times$  129SV background, have been crossed with C57BL/6, and homozygous mice were obtained by backcross. The KO and wild-type (WT) generations were housed in a pathogen-free facility, and procedures were approved by the Animal Care Board of the Istituto Superiore di Sanità. CD1 mice were obtained from The Jackson Laboratory.

### Monoclonal Abs and flow cytometry

For phenotypical analyses, the following surface anti-mouse Abs from BD Biosciences were used: anti-CD4-FITC (H129.19), anti-CD4-PE (RM4-5), anti-CD25-PE (PC61), anti-CD45RB-biotin (16A), anti-rabbit-FITC, anti-CD62L-biotin (MEL14), and anti-CTLA-4-biotin (9H10). Biotinylated mAbs were detected with Streptavidin Red 670. Rabbit anti-mouse Foxp3 Ab was purchased from Abcam (catalog no. Ab15590). For intracellular staining of CTLA-4-PE and Foxp3, cells were fixed and permeabilized with the Cytofix/Cytoperm kits (BD Biosciences). Intracellular staining with the anti-mouse Foxp3-PE (FJK-16s) and the anti-human Foxp3-PE (hFOXY and PCH101; eBioscience) were performed with the mouse/rat Foxp3 Staining set and the PE anti-human Foxp3 staining set, respectively, following the manufacturer's instructions. Human T cells were stained with anti-CD4-FITC (RPA-T4) and anti-CD25-PE (2A3) conjugated Abs (BD Biosciences). Viable cells were selected for analysis based on forward and side scatter light properties. Data were analyzed with CellQuest software (BD Biosciences).

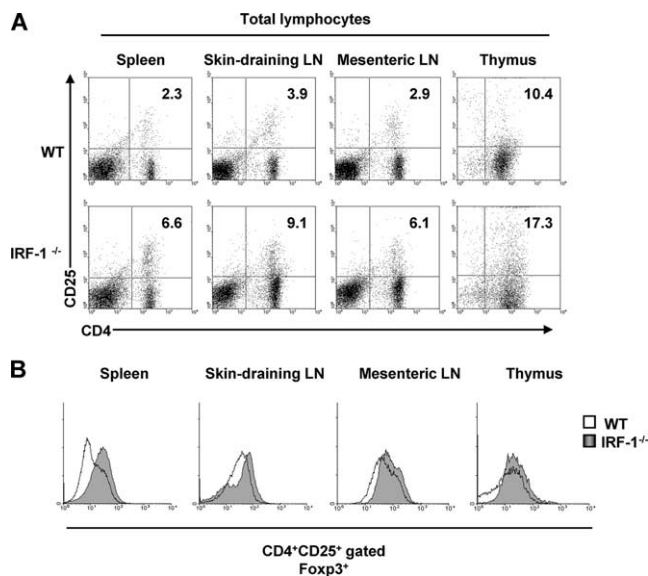


**FIGURE 1.** CD4<sup>+</sup>CD25<sup>+</sup> Treg cells are increased in IRF-1<sup>-/-</sup> mice and display more increased Foxp3 expression than WT Treg cells. Freshly isolated lymphocytes were obtained from the indicated lymphoid organs of WT or IRF-1<sup>-/-</sup> mice. **A**, Cells were double stained for CD4 and CD25 and CD4/CD25 flow cytometric plots were gated on live cells. Value in upper right quadrant indicates the percentage of CD4<sup>+</sup>CD25<sup>+</sup> Treg cells. **B**, Cells were triple stained for CD4, CD25, and Foxp3. Foxp3 plots were gated on CD4<sup>+</sup>CD25<sup>+</sup> cells. Data are representative of six mice per group analyzed in four independent experiments.

### Cell lines and isolation of mouse and human primary CD4<sup>+</sup> and CD4<sup>+</sup>CD25<sup>+</sup> Treg cells

Jurkat T cells (clone 1E6; American Type Culture Collection), where indicated, were treated overnight with 10 ng/ml human rIFN- $\gamma$  (PeproTech). Lymph node, spleen, and thymus cell suspensions and isolation of mouse CD4<sup>+</sup>CD25<sup>+</sup> Treg cells and DC from WT and IRF-1<sup>-/-</sup> mice were performed as previously described (33). PBMC from healthy donors were isolated by Ficoll-Hypaque gradient, and the CD4<sup>+</sup> T cell population purified by negative selection using magnetic beads (Miltenyi Biotec). CD25<sup>+</sup> T cells were isolated by positive selection using anti-CD25 microbeads (Miltenyi Biotec). The purity of CD4<sup>+</sup>CD25<sup>-</sup> T cell fractions was always >96%, and CD4<sup>+</sup>CD25<sup>+</sup> Treg cells were pure at 75–90%. CD4<sup>+</sup>CD25<sup>+</sup> Treg cells were treated with 10 ng/ml human rIL-2 (PeproTech) and stimulated with precoat anti-human CD3 mAbs (UCHT1; BD Biosciences) to further enhance Foxp3 expression.

### Semiquantitative and real-time quantitative RT-PCR

Total RNA was extracted from magnetically purified CD4<sup>+</sup>CD25<sup>-</sup> T cells, CD4<sup>+</sup>CD25<sup>+</sup> Treg cells, or from inTreg cells by using RNeasy Mini kit (Qiagen). RNA was DNase I digested (Roche) and reverse transcribed as previously described (33). Semiquantitative nonsaturating PCR was performed using specific murine primer pairs and conditions already described (26, 33). For Foxp3, primers 5'-TCTTGCCAAGCTGGAAGACT-3' and 5'-AGCTGATGCATGAAGTGTGG-3' were used at 57°C for 30 cycles. Quantitative PCR was performed in duplicate by the real-time fluorescence detection method with the fluorescent DNA binding dye SYBR Green (Power SYBR Green PCR master kit; Applied Biosystems) using an ABI PRISM 7000 sequence detection system (Applied Biosystems) according to the manufacturer's protocol. Primers and conditions used for real-time PCR have been previously described (36, 37). Each of the primer set gave a unique product. Transcript levels were normalized by GAPDH.

### Suppression assay

For suppression assay, an increasing number of freshly isolated or TGF- $\beta$ -induced Treg cells (inTreg) were seeded in 96-well round-bottom microtiter plates with 10<sup>5</sup> CD4<sup>+</sup>CD25<sup>-</sup> T cells and 0.5  $\times$  10<sup>5</sup> allogeneic APC. Cells were incubated with 0.5  $\mu$ g/ml anti-mouse CD3 mAbs (BD Biosciences) for 96 h in complete medium. Neutralizing purified anti-mouse IL-10 (JES5-16E3) or isotype control Abs (both from BD Biosciences) were

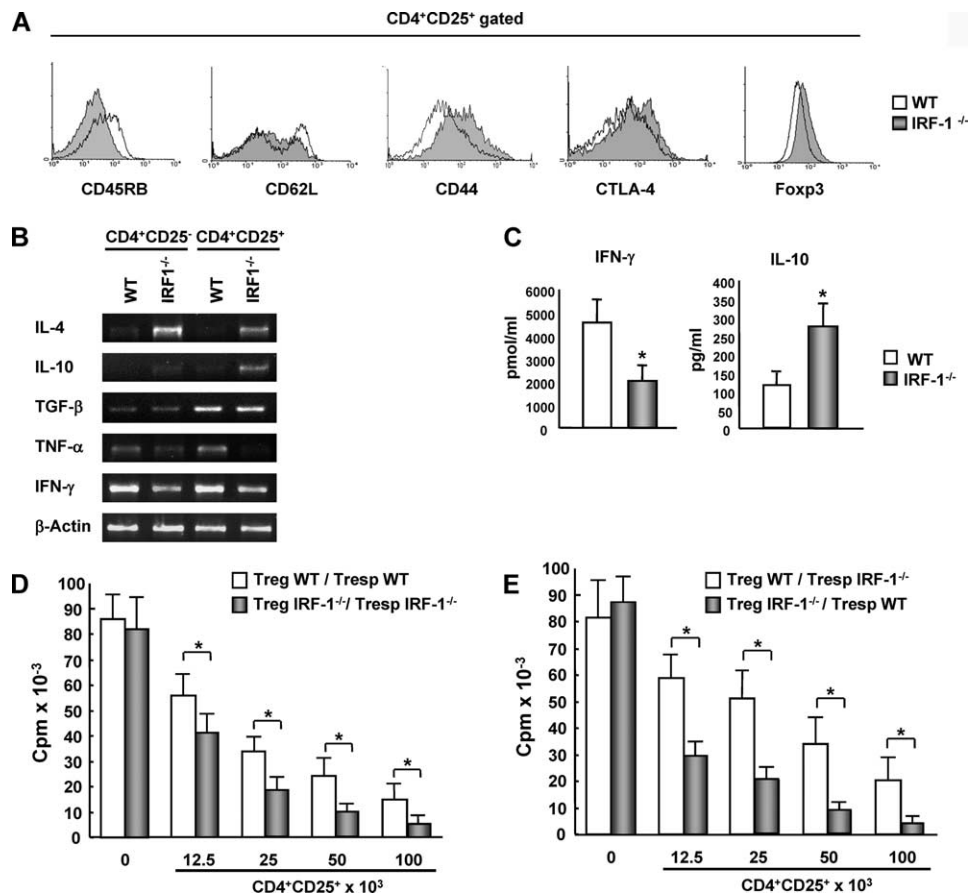


**FIGURE 2.** CD4<sup>+</sup>CD25<sup>+</sup> Treg cells isolated from IRF-1<sup>-/-</sup> mice show a high tolerogenic phenotype and are functionally more suppressive than WT Treg cells. *A*, Freshly isolated, magnetically sorted splenic CD4<sup>+</sup>CD25<sup>+</sup> Treg cells were triple stained for CD4 and CD25, and alternatively for CD45RB, CD62L, CD44, CTLA-4, and Foxp3 and analyzed by flow cytometry. Data are representative of six mice per group analyzed in four independent experiments. *B*, Total RNA was extracted from isolated CD4<sup>+</sup>CD25<sup>+</sup> Treg and CD4<sup>+</sup>CD25<sup>-</sup> T cells from IRF-1<sup>-/-</sup> and WT mice and assayed by nonsaturating RT-PCR for expression of the indicated cytokines. Representative data from three independent experiments are shown. *C*, Secreted amounts of IFN- $\gamma$  and IL-10 were determined by ELISA, in the supernatants of 0.5  $\mu$ g/ml soluble anti-CD3-stimulated CD4<sup>+</sup>CD25<sup>+</sup> Treg cells and CD4<sup>+</sup>CD25<sup>-</sup> T cells cocultured with allogeneic APC. Data shown are mean  $\pm$  SD ( $n = 9$  mice per group). \*,  $p < 0.01$ . *D* and *E*, Freshly isolated CD4<sup>+</sup>CD25<sup>+</sup> Treg cells from IRF-1<sup>-/-</sup> and WT mice were plated in 96-well plates at different concentrations with fixed amounts of autologous WT or IRF-1<sup>-/-</sup> CD4<sup>+</sup>CD25<sup>-</sup> responder T cells ( $10^5$ ) and vice versa with allogeneic APC ( $0.5 \times 10^5$ ) and with 0.5  $\mu$ g/ml soluble anti-CD3 mAbs for 96 h. [<sup>3</sup>H]Thymidine incorporation was measured. Data are expressed as mean  $\pm$  SD ( $n = 9$  mice per group). \*,  $p < 0.05$ .

added to the culture medium at 10  $\mu$ g/ml. Cells were pulsed with 1  $\mu$ Ci of [<sup>3</sup>H]thymidine for the last 16 h of culture.

#### Cytokine assay

Freshly isolated, magnetically sorted CD4<sup>+</sup>CD25<sup>+</sup> Treg cells and CD4<sup>+</sup>CD25<sup>-</sup> responder T cells were cultured with allogeneic APC and 0.5  $\mu$ g/ml anti-mouse CD3 (ratio 1:0.5; BD Biosciences) for 48 h in complete medium. Amounts of IL-10 and IFN- $\gamma$  proteins secreted into the medium were determined using the Quantikine ELISA kits (R&D Systems).

#### In vitro TGF- $\beta$ induction of mouse and human CD4<sup>+</sup>CD25<sup>+</sup> Treg cells

Freshly isolated CD4<sup>+</sup>CD25<sup>-</sup> T cells from spleens of WT and IRF-1<sup>-/-</sup> mice were cultured with allogeneic APC (ratio 1:0.5) and 0.5  $\mu$ g/ml purified anti-mouse CD3 mAbs (145-2C11; BD Biosciences) alone or with 2 ng/ml TGF- $\beta$ 1 (PeproTech) for 3 days in RPMI 1640 medium (BioWhittaker) supplemented with 10% heat-inactivated FCS, 50 mM 2-ME, 10 mM HEPES, 1 mM sodium pyruvate, 1 mM nonessential amino acid, 100 U/ml penicillin, and 100  $\mu$ g/ml streptomycin (complete medium). Freshly isolated magnetically sorted human CD4<sup>+</sup>CD25<sup>-</sup> T cells were cultured into anti-CD3 mAb (UCHL1) precoated plates with anti-CD28 mAbs (37407.111; both from R&D Systems) alone or with 2 ng/ml TGF- $\beta$  (PeproTech) for 3 days in complete medium.

#### Retroviral infection

The coding sequence of murine IRF-1 cDNA (1 kb) was subcloned from pcDNA3.1 into pMSCV MigR1-CD8 retroviral vector, which was a gift of

Dr. K. Ozato (National Institutes of Health, Bethesda, MD). The vector DNA with insert (MigR1-IRF-1-CD8) or the empty vector (MigR1-EV-CD8) were transfected into the  $\psi$ MX-E packaging cell line using Fugene 6 (Roche), according to the manufacturer's protocol. Retrovirus-containing supernatant of the transfected packaging cells at 32°C was collected after a 36-h culture.

Freshly isolated IRF-1<sup>-/-</sup> CD4<sup>+</sup>CD25<sup>-</sup> T cells were activated using 0.5  $\mu$ g/ml plate-bound anti-CD3 (145-2C11) and 1  $\mu$ g/ml anti-CD28 Abs (37.51) (BD Biosciences). After 24 h of activation, cells were infected by resuspending cells in retrovirus-containing supernatants supplemented with 8  $\mu$ g/ml polybrene (Sigma-Aldrich), followed by two steps of spinoculations for 90 min at 2500 revolutions per minute. After 6 h, cells were washed and plated into anti-CD3 precoated plates and cultured for 72 h at 37°C in the presence of 2 ng/ml TGF- $\beta$  and anti-CD28 Abs. Retroviral transduction led to expression of CD8<sup>+</sup> cells in 30–60% of infected cells.

#### Cloning of the human foxp3 promoter

Genomic sequences spanning the 5' untranslated region of the human *foxp3* gene (31) were analyzed by using the Genomatix software. A fragment of 304 bp encompassing the transcription start site of the human *foxp3* gene promoter (38) and containing a IRF-E spanning from -234 to -203 bp upstream of the transcription start site was amplified from genomic DNA extracted from PBMC of healthy individuals. A fragment of 304 bp containing the IRF-E spanning from -234 to -273 bp upstream of the transcription start was amplified from genomic DNA extracted from PBL of healthy individuals using a QIAamp DNA extraction kit (Qiagen) by PCR using the PfuTurbo DNA polymerase (Stratagene) and the following primers: forward 5'-AAG GTA CCC TCT GTG GTG AGG GGA



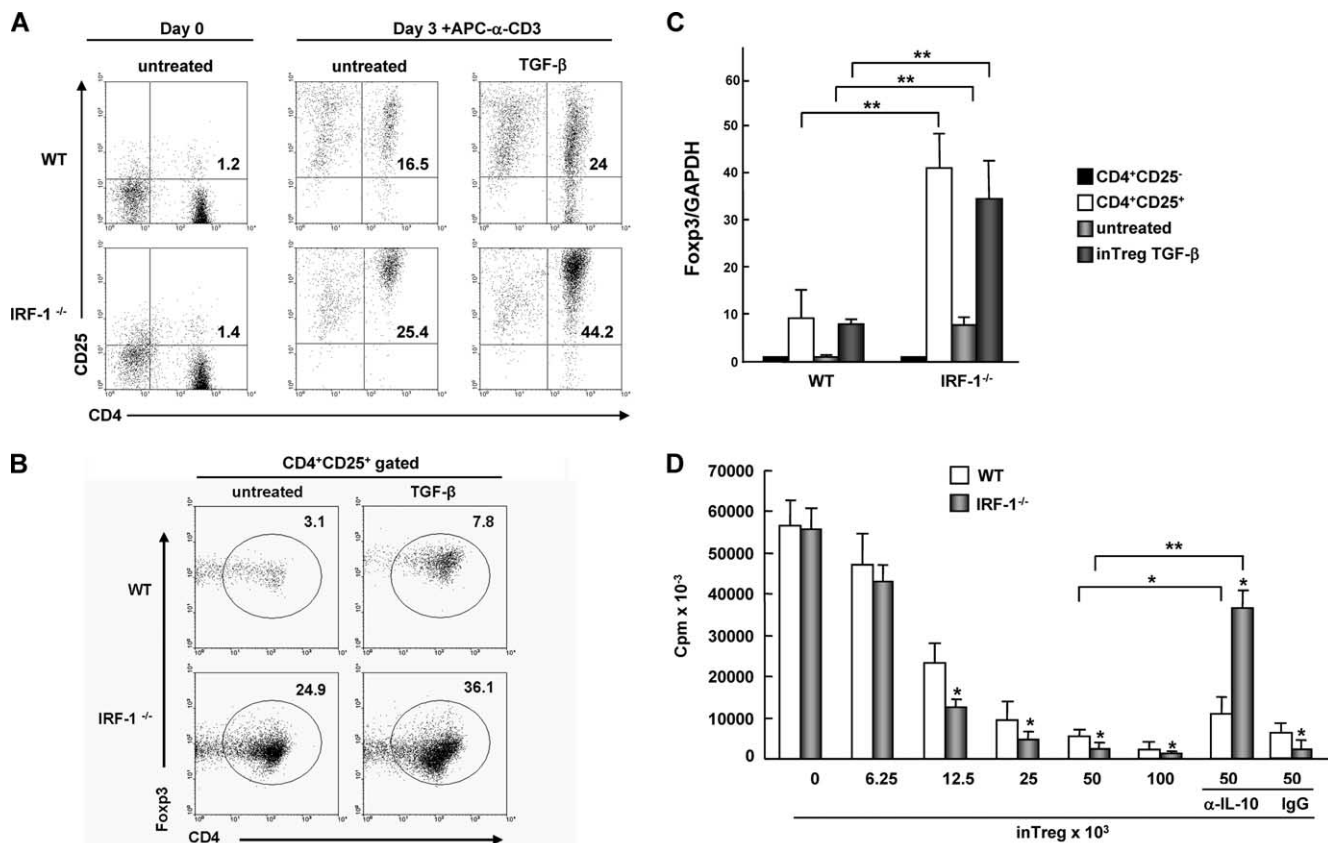


**FIGURE 3.** CD4<sup>+</sup>CD25<sup>-</sup> T cells isolated from IRF-1<sup>-/-</sup> mice show high bent to convert into CD4<sup>+</sup>CD25<sup>+</sup> Treg cells and are functionally more suppressive than WT cells. Freshly isolated CD4<sup>+</sup>CD25<sup>-</sup> T cells were induced with allogeneic APC and 0.5 μg/ml soluble anti-CD3 mAbs and cultured in presence or absence of 2 ng/ml TGF-β for 72 h (inTreg). Cells were triple stained for CD4, CD25, and Foxp3 and analyzed by FACS before and after 72 h. Results are shown as CD4<sup>+</sup>CD25<sup>+</sup> T cells (A) and CD4<sup>+</sup>Foxp3<sup>+</sup> T cells (B) and value in top right quadrant indicates the percentage of CD4<sup>+</sup>CD25<sup>+</sup> T cells in A and CD4<sup>+</sup>Foxp3<sup>+</sup> T cells in B. Data are representative of *n* = 6 mice per group analyzed in three independent experiments. C, IRF-1<sup>-/-</sup> and WT TGF-β-treated inTreg cells together with magnetically isolated IRF-1<sup>-/-</sup> and WT CD4<sup>+</sup>CD25<sup>+</sup> Treg cells were collected, and total RNA extracted and reverse transcribed. cDNAs were subjected to real-time PCR and analyzed for Foxp3 and GAPDH expression. Data are normalized on GAPDH values and expressed as mean ± SD. \*\*, *p* < 0.01. D, IRF-1<sup>-/-</sup> and WT TGF-β-treated inTreg cells were plated in 96-well plates at different concentrations with fixed amounts of syngeneic CD4<sup>+</sup>CD25<sup>-</sup> T cells and 0.5 × 10<sup>5</sup> allogeneic APC and with 0.5 μg/ml soluble anti-CD3 mAbs for 96 h. Saturating amounts of anti-IL-10 neutralizing mAbs or isotype control Abs were added to the culture medium as indicated. Data are mean ± SD (*n* = 6 mice per group). \*, *p* < 0.05; and \*\*, *p* < 0.01.

AGA A-3' and reverse 5'-TTG AGC TCC TGG CTT GTG GGG AAA CTG TC-3'. *KpnI* and *SacI* restriction enzyme sites were introduced into the forward and the reverse primer (underlined bases), respectively. PCR products were purified, digested, and incorporated into the luciferase reporter plasmid pGL3-Basic Vector (Promega). The mutated Foxp3 construct was obtained from the WT construct by site-directed mutagenesis of the IRF-E site by using the QuikChange site-directed mutagenesis kit (Stratagene). The sequence of the primer used to introduce specific mutations was 5'-CCA AAA TTT CAA AAT GTC CAT CTA AGT CTC A-3'. Constructs were verified by sequencing the inserts and flanking regions of plasmids.

#### DNA affinity binding assay and immunoblotting

Nuclear protein extracts from Jurkat, human or mouse freshly isolated CD4<sup>+</sup>CD25<sup>+</sup> Treg cells, CD4<sup>+</sup>CD25<sup>-</sup> T cells, and inTreg cells as well as DNA affinity binding assays were performed as described (39). Complementary biotinylated oligonucleotides sequences are the following: Foxp3 IRF-E, CCA AAA TTT CAA AAT TTC CGT TTA AGT CTC A; mutant IRF-E, CCA AAA TTT CAA AATGTC CAT CTA AGT CTC A; C13, GAT CAA CTG AAA CTG AAA CTG AAA CTGA; and β-casein, GAT TTC TAG GAA TTC AAT C. Eluted material was separated onto 10% SDS-PAGE followed by immunoblotting with anti-IRF-1 Abs (sc-497 and sc-640; Santa Cruz Biotechnology).

#### Transfection of Jurkat T cells, nucleofection of CD4<sup>+</sup> primary T cells, and luciferase assay

Jurkat T cells were transfected with 1 μg of each plasmid construct and 0.1 μg of *Renilla* luciferase control vector (pRL-Act *Renilla*) by using Eugene

6 (Roche). Where indicated, IRF-1- or IRF-2-expressing vector (39) were cotransfected. Twenty-four hours later, firefly and *Renilla* luciferase activities were measured by the Dual Luciferase Reporter Assay System (Promega). Transfections were performed in triplicates for each construct and repeated at least three times. Data were normalized to the activity of *Renilla* luciferase. Primary CD4<sup>+</sup> T cells in PBS supplemented with 0.5% BSA were incubated overnight at 4°C then 2.5 μg of the Foxp3 promoter luciferase reporter vector, 2 μg of IRF-1 expression vector, 0.2 μg of *Renilla* luciferase control vector, and 0.5 μg of pEGFP plasmid (Amaxa) were added to 5 × 10<sup>6</sup> CD4 T cells resuspended in 100 μl of Nucleofector solution (Amaxa) and electroporated using the U-14 and X-01 program of the Nucleofector specific for untouched human and murine CD4<sup>+</sup> T cells, respectively. Transfection efficiency was monitored in all samples by FACS analysis of GFP fluorescence and was ranging from 30 to 50% for human cells depending on the donor in three independent experiments and from 15 to 25% for mouse cells. After 24 h, luciferase activity was measured as described.

#### Chromatin immunoprecipitation (ChIP)

ChIP assays were performed as previously described (40). Briefly, CD4<sup>+</sup>CD25<sup>-</sup> and CD4<sup>+</sup>CD25<sup>+</sup> Treg cells were magnetically sorted from PBMC of healthy donors or mouse spleens. Human CD4<sup>+</sup>CD25<sup>+</sup> Treg cells were stimulated with anti-CD3 mAbs and 10 ng/ml human rIL-2 for 12 h. Formaldehyde (final concentration, 1%) was then added to cross-link proteins and DNA. The cell lysates were sonicated and immunoprecipitated with normal rabbit serum (BD Biosciences) or anti-IRF-1 Abs (Santa Cruz Biotechnology). The immunoprecipitated DNA was eluted and amplified by real-time PCR using an ABI 7700 (Applied Biosystems). Values were

normalized to corresponding input control and are expressed as fold enrichment relative to normal rabbit serum for each experiment. The sequence of specific primers used for amplification of the *foxp3* gene surrounding the IRF-E binding sites was 5'-GTG GTG AGG GGA AGA AAT CA-3' and 3'-GAT GAG TGT GTG CGC TGA TAA-5'.

Quantitative PCR was performed in duplicate by the real-time fluorescence detection method with the fluorescent DNA binding dye, SYBR Green (Power SYBR Green PCR master kit; Applied Biosystems) using an ABI PRISM 7000 sequence detection system (Applied Biosystems), according to the manufacturer's protocol. The primers gave a unique product at 179 bp.

### Statistical analysis

Student's *t* tests were used to calculate differences between the groups. Differences in values of  $p \leq 0.05$  were considered significant.

## Results

### *CD4<sup>+</sup>CD25<sup>+</sup> Treg from IRF-1<sup>-/-</sup> mice are increased and functionally more suppressive than WT Treg cells*

The distribution and the phenotype of CD4<sup>+</sup>CD25<sup>+</sup>Foxp3<sup>+</sup> Treg in lymphoid organs of IRF-1<sup>-/-</sup> mice were determined by flow cytometry. As shown in Fig. 1A, the number of ex vivo double positive CD4<sup>+</sup>CD25<sup>+</sup> cells was significantly increased in spleens and skin draining and mesenteric lymph nodes (2.8-, 2.3-, and 2.1-fold increase, respectively), and to a lesser extent, in thymus (1.6-fold increase) of IRF-1<sup>-/-</sup> mice as compared with WT mice. Consistently with previous reports (23, 41), no differences in CD4<sup>+</sup> T cell and total cell numbers in all lymphoid organs from WT or IRF-1<sup>-/-</sup> mice were found (data not shown). Strikingly, intracellular analysis of Foxp3 expression showed that this factor was increasingly expressed in CD4<sup>+</sup>CD25<sup>+</sup> Treg cells from spleens as well as from other lymphoid organs of IRF-1<sup>-/-</sup> mice (Fig. 1B).

Next, FACS analysis of splenic magnetically sorted CD4<sup>+</sup>CD25<sup>+</sup> Treg cells was performed to evaluate the expression of activation markers. As shown in Fig. 2A, IRF-1<sup>-/-</sup> Treg cells were to a large extent CD45RB<sup>low</sup>CD62L<sup>low</sup>CD44<sup>high</sup>CTLA-4<sup>high</sup>Foxp3<sup>high</sup> characteristic of a marked activated and differentiated phenotype.

Because there is accumulating evidence that activity of CD4<sup>+</sup>CD25<sup>+</sup> Treg cells in vivo involves some immunosuppressive cytokines (9–12), we also compared the cytokine profile of IRF-1<sup>-/-</sup> CD4<sup>+</sup>CD25<sup>+</sup> Treg cells with the profile of WT counterparts (Fig. 2B). Lower levels of proinflammatory cytokines, such as TNF- $\alpha$  and IFN- $\gamma$ , whereas higher levels of IL-4 were expressed in CD4<sup>+</sup>CD25<sup>+</sup> Treg cells as well as in CD4<sup>+</sup>CD25<sup>-</sup> T lymphocytes from KO as compared with WT cells (Fig. 2B). Notably, only IRF-1<sup>-/-</sup> Treg cells showed a clear-cut increase in the expression of IL-10. By contrast, TGF- $\beta$  was expressed at similar levels in CD4<sup>+</sup>CD25<sup>+</sup> Treg cells from both IRF-1<sup>-/-</sup> and WT mice (Fig. 2B). Accordingly with mRNA data, IL-10 secretion in supernatants of TCR-stimulated CD4<sup>+</sup>CD25<sup>+</sup> cocultures from IRF-1<sup>-/-</sup> mice was significantly increased (3-fold), whereas IFN- $\gamma$  secretion was decreased (2.5-fold) compared with cocultures from WT mice (Fig. 2C).

As the functional hallmark of Treg cells is their ability to suppress the expansion of effector T cells, we next evaluated this activity performing suppression assays (1–3, 8). Importantly, CD4<sup>+</sup>CD25<sup>+</sup> Treg cells from IRF-1<sup>-/-</sup> mice were found significantly more efficient than WT Treg cells in suppressing the proliferation of syngeneic CD4<sup>+</sup>CD25<sup>-</sup> responder T cells in a dose-dependent fashion (Fig. 2D). Next, to verify whether IRF-1<sup>-/-</sup> Treg cells suppression ability was retained vs WT responder T cells, we performed suppression assays using IRF-1<sup>-/-</sup> Treg and WT responders and vice versa. As shown in Fig. 2E, the sup-

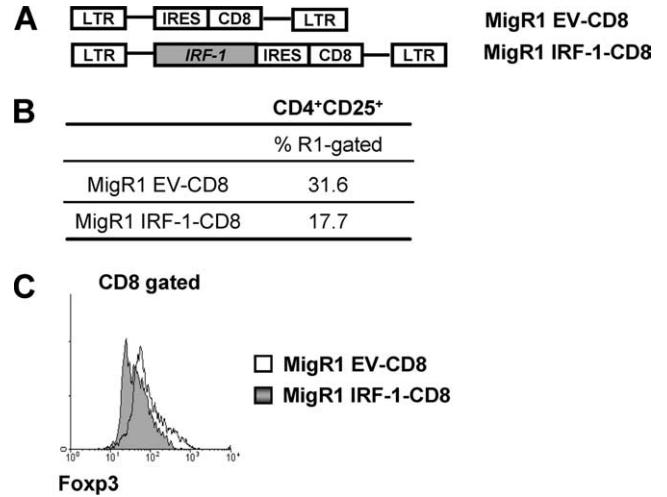


**FIGURE 4.** IRF-1 impairs CD4<sup>+</sup>CD25<sup>+</sup> Treg cell induction by TGF- $\beta$ . **A**, Bicistronic retroviral vector encoding IRF-1 and CD8 (MigR1 IRF-1-CD8) under the control of an internal ribosomal entry site or CD8 alone (MigR1 EV-CD8). **B**, CD4<sup>+</sup>CD25<sup>-</sup> T cells isolated from IRF-1<sup>-/-</sup> mice were activated with 1  $\mu$ g/ml soluble anti-CD3 and anti-CD28 mAbs and infected with the retrovirus expressing the CD8 or the IRF-1/CD8 proteins and TGF- $\beta$ -induced for 72 h. Cells were stained for CD4 and CD25 markers and analyzed by flow cytometry. Representative data from four independent experiments are shown. **C**, CD4<sup>+</sup>CD25<sup>-</sup> T cells isolated from IRF-1<sup>-/-</sup> mice were infected with the retrovirus expressing the CD8 or the IRF-1/CD8 proteins and TGF- $\beta$ -induced for 72 h. Cells were stained for CD8 and Foxp3 and analyzed by flow cytometry. Representative data from four independent experiments are shown.

pressive activity of IRF-1<sup>-/-</sup> Treg cells toward WT responders was dose-dependently increased, as well.

### *IRF-1<sup>-/-</sup> CD4<sup>+</sup>CD25<sup>-</sup> T cells show high bent to convert into CD4<sup>+</sup>CD25<sup>+</sup> Treg cells*

It has been reported in mice and human that TGF- $\beta$  promotes the induction of peripheral CD4<sup>+</sup>CD25<sup>-</sup> T cells into CD4<sup>+</sup>CD25<sup>+</sup> Treg cells (iTreg), that acquire Foxp3 expression and regulatory functions (14–20). To investigate the potential of CD4<sup>+</sup>CD25<sup>-</sup> T cells from IRF-1<sup>-/-</sup> mice to acquire a regulatory phenotype compared with WT cells, CD4<sup>+</sup>CD25<sup>-</sup> T cells were magnetically isolated from spleen of IRF-1<sup>-/-</sup> and WT mice, cocultured with APC and stimulated with anti-CD3 mAbs in presence or absence of TGF- $\beta$ . After 3 days, FACS analysis revealed that, in presence of TGF- $\beta$ , 44.2% of CD4<sup>+</sup>CD25<sup>+</sup> iTreg cells were generated in the coculture of CD4<sup>+</sup>CD25<sup>-</sup> T cells from IRF-1<sup>-/-</sup> mice, whereas only 24% of double positive cells were detected in the corresponding coculture from WT mice (Fig. 3A). Notably, even in absence of TGF- $\beta$ , 25.4% CD4<sup>+</sup>CD25<sup>+</sup> iTreg were generated in the coculture of CD4<sup>+</sup>CD25<sup>-</sup> T cells from IRF-1<sup>-/-</sup> mice, as compared with 16.5% of Treg cells generated in WT cocultures (Fig. 3A). Importantly, an increased number of CD4<sup>+</sup>CD25<sup>+</sup>-gated Foxp3<sup>+</sup> cells were observed in IRF-1<sup>-/-</sup> iTreg cells in the presence (4.5-fold increase) or in the absence (8-fold increase) of TGF- $\beta$  compared with WT iTreg cells (Fig. 3B). Next, to evaluate quantitatively Foxp3 expression levels in TGF- $\beta$ -induced Treg vs ex vivo freshly purified Treg cells, quantitative real-time PCR was performed. A clear-cut induction of Foxp3 mRNA (4.5-fold increase) was detected in TGF- $\beta$ -treated IRF-1<sup>-/-</sup> cells compared with WT cells (Fig. 3C). Of note, these levels were comparable with those present in freshly isolated IRF-1<sup>-/-</sup> CD4<sup>+</sup>CD25<sup>+</sup> cells. Strikingly, also untreated IRF-1<sup>-/-</sup> T cells showed higher levels of

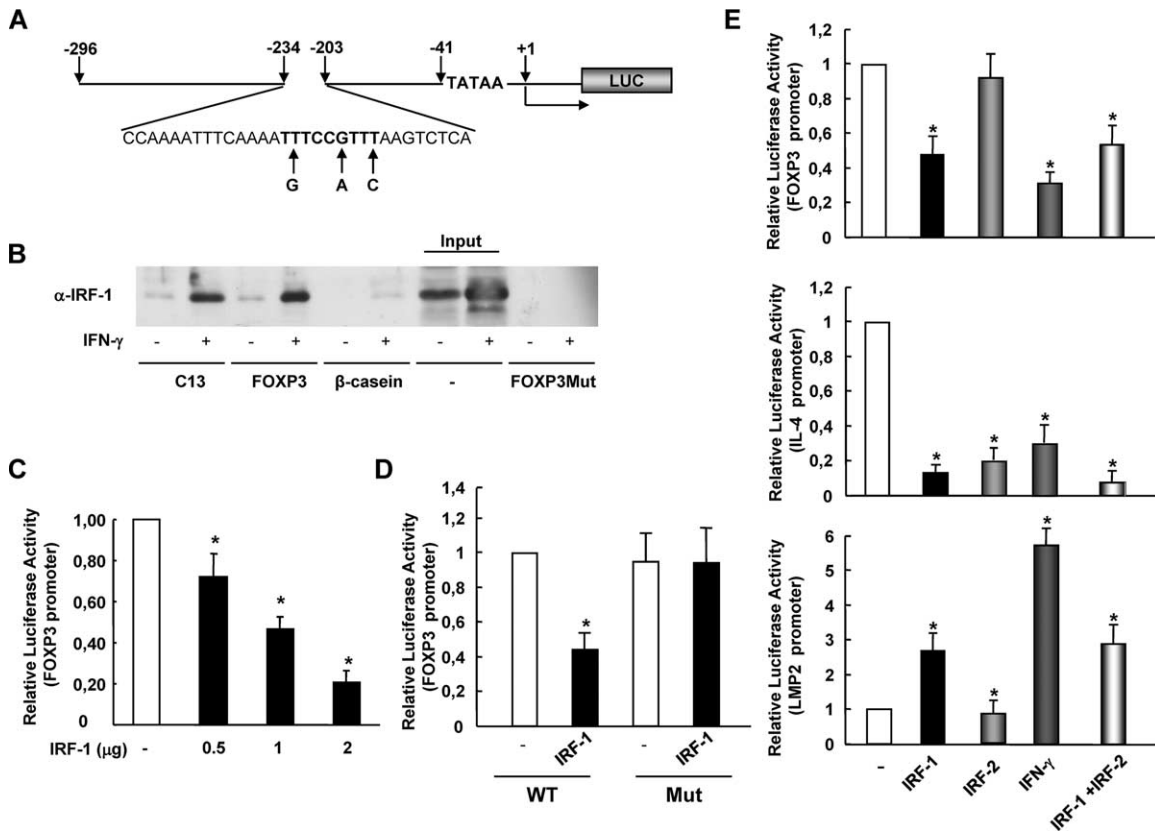


**FIGURE 5.** IRF-1 specifically binds IRF-E on the human *foxp3* gene promoter and inhibits its transcriptional activity. *A*, Schematic representation of human *foxp3* gene promoter (human accession no. AF235097). The sequence shown in bold is the IRF-E. Arrows indicate substitutions introduced in mutated Foxp3 oligonucleotides and in the Foxp3 promoter vector used in pull-down and luciferase assays, respectively. *B*, Pull-down assays were performed incubating nuclear extracts from Jurkat T cells untreated or treated overnight with 10 ng/ml human rIFN- $\gamma$  together with C13, WT Foxp3,  $\beta$ -casein, or mutated Foxp3 oligonucleotides. The DNA-bound IRF-1 was detected by immunoblotting. Representative data from three independent experiments are shown. *C* and *D*, Luciferase assays were performed in Jurkat T cells transfected with the *Renilla* luciferase vector plus the luciferase vector containing *foxp3* gene promoter and increasing concentrations of IRF-1 expression vector (*C*) and with WT and mutated luciferase vector containing *foxp3* gene promoter (*D*). Results are mean  $\pm$  SD ( $n = 3$ ; \*,  $p < 0.05$ ). *E*, Luciferase assays were performed in Jurkat T cells transfected with the *Renilla* luciferase vector plus the *foxp3* (upper), *il4* (middle), and *lmp2* (lower) gene promoters and expression vectors IRF-1, IRF-2, or both. Where indicated, cells were treated overnight with 10 ng/ml human rIFN- $\gamma$ . Results are mean  $\pm$  SD ( $n = 6$ ; \*,  $p < 0.05$ ).

Foxp3 mRNA than WT untreated cells (6-fold increase) and similar to levels present in freshly purified WT CD4<sup>+</sup>CD25<sup>+</sup> Treg cells (Fig. 3C).

The functionality of CD4<sup>+</sup>CD25<sup>+</sup>Foxp3<sup>+</sup> inTreg cells was then assessed by suppression assays. As shown in Fig. 3D, TGF- $\beta$ -treated IRF-1<sup>-/-</sup> inTreg cells were significantly more effective than the WT counterpart cells in suppressing proliferation of effector T cells in a dose-dependent way. Interestingly, a saturating amount of anti-IL-10 mAbs neutralized the suppression ability of inTreg cells from both IRF-1<sup>-/-</sup> and WT mice even though the effect was much more marked in IRF-1<sup>-/-</sup> inTreg cells. Control Abs did not exhibit any effect.

#### Restoring IRF-1 expression in IRF-1<sup>-/-</sup> CD4<sup>+</sup>CD25<sup>-</sup> T cells impairs their differentiation into CD4<sup>+</sup>CD25<sup>+</sup>Foxp3<sup>+</sup> cells

To address the specificity of IRF-1 role in differentiation of CD4<sup>+</sup>CD25<sup>+</sup> Treg cells from CD25<sup>-</sup> cells, we investigate whether forced expression of IRF-1 in CD4<sup>+</sup>CD25<sup>-</sup> IRF-1<sup>-/-</sup> T cells could rescue the WT phenotype. To such purpose, bicistronic retroviral vectors expressing murine IRF-1 and human CD8 protein as surface marker (MigR1 IRF-1-CD8) or CD8 alone (MigR1 EV-CD8) were generated (Fig. 4A). Splenic CD4<sup>+</sup>CD25<sup>-</sup> cells from IRF-1<sup>-/-</sup> mice were stimulated with plate-bound anti-CD3 and anti-CD28 Abs and infected with either retrovirus. As shown

in Fig. 4B, 31.6% of MigR1 EV-CD8 CD4<sup>+</sup> retrovirus-infected cells were CD25<sup>+</sup>, by contrast only 17.7% of MigR1 IRF-1-CD8 retrovirus-infected cells were double positive. Consistently, Foxp3 expression in CD8<sup>+</sup>-gated cells was significantly decreased in MigR1 IRF-1-CD8-infected cells as compared with those infected with MigR1 EV-CD8 vectors (Fig. 4C), strongly supporting the evidence that IRF-1 specifically impairs CD4<sup>+</sup>CD25<sup>+</sup> cell differentiation.

#### IRF-1 binds an IRF-E on the Foxp3 core promoter and inhibits its transcriptional activity

To shed light on the molecular mechanisms responsible for the striking effect exerted by IRF-1 on the development and function of CD4<sup>+</sup>CD25<sup>+</sup> Treg cells, we investigated whether IRF-1, which is a regulator of key immunomodulatory genes (21), could directly regulate the *foxp3* gene promoter activity. The proximal promoter of human *foxp3* gene has been recently characterized and localized at -511/+176 bp upstream of the 5' untranslated region (38). By the Genomatix software, we analyzed this region and found an IRF-E spanning from -234 to -203 bp (Fig. 5A). This region has been found highly homologous to mouse and rat *foxp3* promoter, and of note, the IRF-E is perfectly conserved between humans and these species (38). To determine whether IRF-1 could bind this sequence, DNA affinity purification assays were performed with

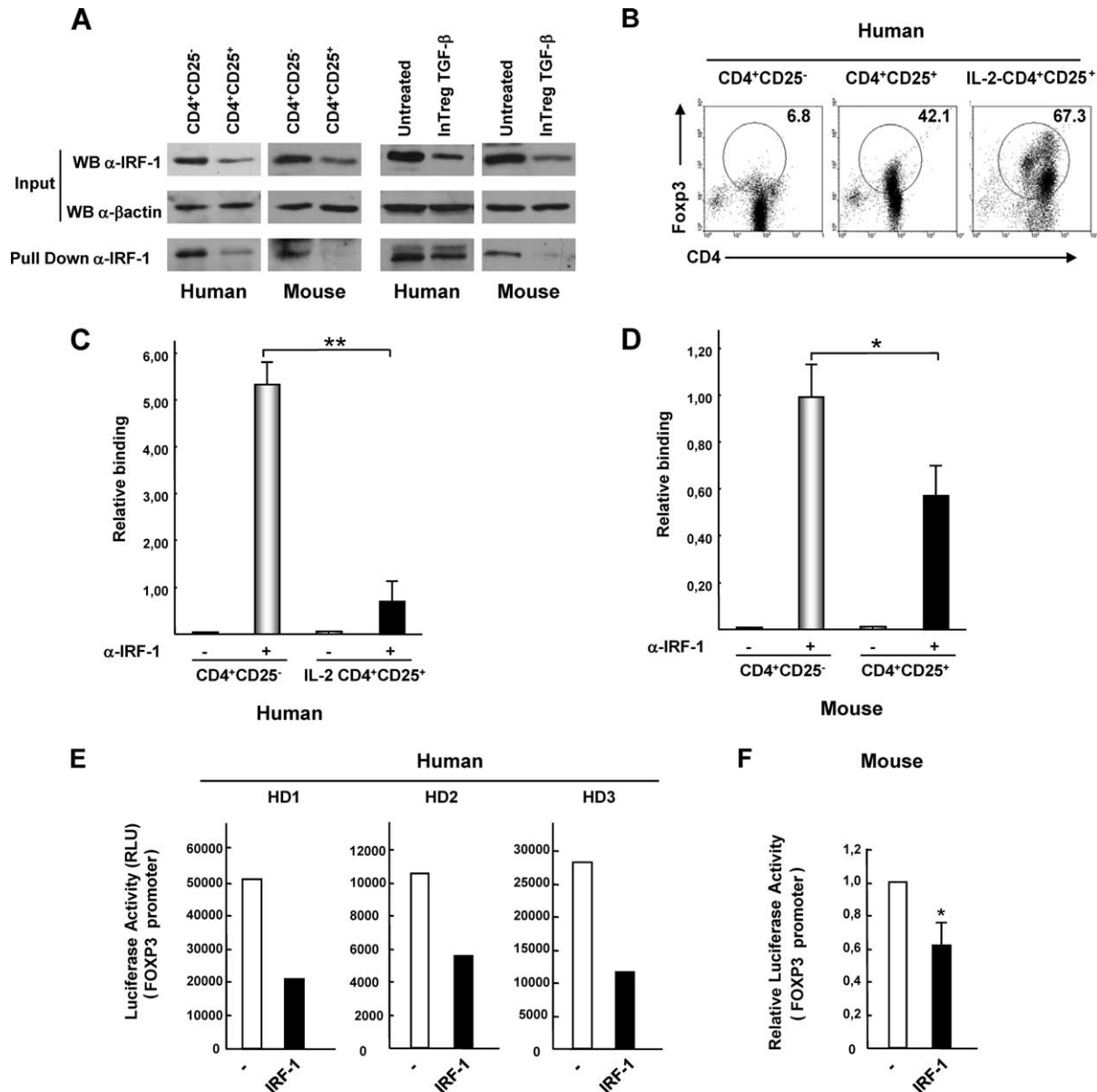


**FIGURE 6.** IRF-1 is down-regulated in primary CD4<sup>+</sup>CD25<sup>+</sup> Treg cells and in TGF-β-induced T cells and binds Foxp3 in vitro and in vivo. *A*, Western blot analysis was performed with nuclear extracts from primary CD4<sup>+</sup>CD25<sup>-</sup> and CD25<sup>+</sup> T cells magnetically isolated from PBMC of healthy donors (HD) or mouse spleens (*left*), and from TCR-stimulated CD4<sup>+</sup>CD25<sup>-</sup> cells cultured with 1 μg/ml soluble anti-CD28 mAbs, in the presence (inTreg) or absence (untreated) of TGF-β for 72 h (*right*). Pull-down assays were performed incubating the same extracts with Foxp3 oligonucleotides. The DNA-bound IRF-1 was detected by immunoblotting with anti-human and anti-mouse IRF-1 Abs. Representative data from four independent experiments are shown. *B*, CD4<sup>+</sup>CD25<sup>-</sup> T cells and CD4<sup>+</sup>CD25<sup>+</sup> Treg cells were magnetically sorted from PBMC of healthy donors. CD4<sup>+</sup>CD25<sup>+</sup> Treg cells were stimulated with anti-CD3 mAbs and 10 ng/ml human rIL-2 for 12 h, and Foxp3 expression was determined by FACS analysis. *C* and *D*, ChIP assay was performed in primary CD4<sup>+</sup>CD25<sup>-</sup> and IL-2-treated CD4<sup>+</sup>CD25<sup>+</sup> cells magnetically isolated from PBMC of healthy donors (*C*) or mouse spleens (*D*) using either normal rabbit serum or anti-human and anti-mouse IRF-1 Abs. Quantification of immunoprecipitated DNA fragments was performed by real-time PCR using primers for IRF-E. Values were normalized to corresponding input control and are expressed as fold enrichment relative to normal rabbit serum for each experiment. Results are mean ± SD (\*\*, *p* < 0.01, *n* = 2; \*, *p* < 0.05, *n* = 2). *E* and *F*, Primary CD4<sup>+</sup> T cells were magnetically isolated from PBMC of three healthy donors (HD1, HD2, HD3) (*E*) or mouse spleens (*F*) and nucleofected with the *Renilla* luciferase vector, a pEGFP vector plus the luciferase vector containing the *foxp3* gene promoter and IRF-1 expression vector. (\*, *p* < 0.05, *n* = 3). Luciferase activity was determined 24 h after nucleofection. Data were normalized by activity of *Renilla* luciferase vector.

cell extracts from Jurkat T cells, which display discrete basal levels of IRF-1, and from the same cells treated with IFN-γ to maximally stimulate IRF-1 expression. A total of 200 μg of nuclear extracts was incubated with oligonucleotides containing the WT or the a mutated version of IRF-E whose sequence is indicated in Fig. 5A. The isolated complexes were then examined by immunoblotting against IRF-1. As shown in Fig. 5B, a specific binding of IRF-1 to Foxp3 oligonucleotide was evident. The binding was strongly

stimulated by IFN-γ treatment and, interestingly, it was comparable to that obtained when the same extracts were incubated with a synthetic oligonucleotide corresponding to C13, the canonical IRF-1 consensus sequence (21). IRF-1 binding was highly specific because a mutated version of the Foxp3/IRF-E, or an unrelated oligonucleotide corresponding to the STAT binding site present on the β-casein gene promoter, did not retain any protein from the same extracts. To functionally characterize the specific binding of



IRF-1 to the *foxp3* gene promoter, we cloned the encompassing part of the proximal promoter containing the IRF-E from  $-296$  to  $+7$  bp of *foxp3* gene promoter upstream the luciferase reporter gene. The effect of IRF-1 was evaluated in Jurkat T cells transiently cotransfected with the luciferase reporter gene and increasing doses of an IRF-1-expressing vector. The results indicated that the basal transcriptional activity of the *foxp3* gene promoter was substantially reduced in the presence of IRF-1 and the effect was dose-dependent (Fig. 5C). Conversely, the basal activity of the *foxp3* gene promoter construct mutated in the IRF-E was not affected by IRF-1 overexpression (Fig. 5D).

Interestingly, IRF-2, a repressor of IRF-1 transcriptional activity on most promoters (21), neither affected the promoter activity nor counteracted the inhibitory effect exerted by IRF-1 (Fig. 5E, upper). Where indicated, cells were treated with IFN- $\gamma$  to maximally stimulate IRF-1 expression, and an even more marked suppression of *foxp3* gene promoter activity was achieved (Fig. 5E, upper). Overexpression of other IRFs including IRF-4 or IRF-8 did not modify the *foxp3* basal activity (our unpublished data). As additional control of specificity, we also performed experiments with two luciferase reporter constructs driven by the IRF-E present on the *il4* and *lmp2* gene promoters (Fig. 5E, middle and lower) described to be negatively (42) and positively (43) regulated by IRF-1, respectively. As expected, IRF-1, IRF-2, as well as the IFN- $\gamma$  treatment drastically reduced the transcriptional activity of the *il4* gene promoter, whereas the low molecular mass polypeptide *lmp2* construct was stimulated by IRF-1 and by IFN- $\gamma$  treatment, but it was not affected by IRF-2. All together these results demonstrate the specificity and functional relevance of IRF-1 binding to the *foxp3* proximal promoter.

*Foxp3 is a direct target of IRF-1 in human and mouse primary CD4<sup>+</sup>CD25<sup>-</sup> T cells and CD4<sup>+</sup>CD25<sup>+</sup> Treg cells*

To assess the biological relevance of the reported effects of IRF-1 on Treg development and on the regulation of Foxp3 expression, we performed experiments with primary cells. We first assessed by Western blot IRF-1 expression levels in CD4<sup>+</sup>CD25<sup>+</sup> Treg cells vs CD4<sup>+</sup>CD25<sup>-</sup> T cells magnetically sorted from PBMC of healthy donors or from mice spleens. Strikingly, we found that IRF-1 was down-regulated in double positive cells as compared with CD4<sup>+</sup>CD25<sup>-</sup> T cells both in mouse and human primary cells (Fig. 6A, left). To determine whether IRF-1 binds the Foxp3 oligonucleotides in primary Treg cells, pull-down assays with the same extracts were then performed. As shown in Fig. 6A, left, IRF-1 binding to Foxp3 oligonucleotide was significantly decreased in primary CD4<sup>+</sup>CD25<sup>+</sup> Treg cells compared with CD4<sup>+</sup>CD25<sup>-</sup> T cells from both species. Foxp3 staining of CD4<sup>+</sup>CD25<sup>-</sup> T cells and CD4<sup>+</sup>CD25<sup>+</sup> human Treg cells confirmed that these cells expressed low and high levels of Foxp3, respectively, and Foxp3 expression was further increased by IL-2 treatment (Fig. 6B).

To test whether IRF-1 expression was also down-modulated during the acquisition of Treg cell phenotype upon TGF- $\beta$  treatment, freshly purified TCR-activated CD4<sup>+</sup>CD25<sup>-</sup> T cells from both species were cultured with TGF- $\beta$ , or left untreated, for 3 days and Western blot analysis was performed. As shown in Fig. 6A, right, when cells were cultured in presence of TGF- $\beta$ , IRF-1 expression was substantially decreased, as compared with untreated cells. Pull-down assays revealed that IRF-1 binding to Foxp3 oligonucleotide was decreased in TGF- $\beta$ -treated primary cells compared with untreated cells, as well (Fig. 6A, right). Consistently, FACS analysis of these cultures indicated that  $\sim 35\%$  of TGF- $\beta$ -treated CD4<sup>+</sup> cells were Foxp3<sup>+</sup> in human and  $\sim 10\%$  in mouse TGF- $\beta$  treated cultures, respectively. By contrast, even

though 46.3% of human untreated cells were CD25<sup>+</sup> only 5% were Foxp3<sup>+</sup> (data not shown).

Next, we assessed the in vivo IRF-1 binding to *foxp3* gene in human and mouse primary magnetically sorted CD4<sup>+</sup>CD25<sup>-</sup> T cells and CD4<sup>+</sup>CD25<sup>+</sup> Treg cells, using ChIP assay with anti-IRF-1 Abs. After DNA immunoprecipitation, subsequent real-time PCR amplification of the *foxp3* gene surrounding the IRF-E site showed significant IRF-1 binding to Foxp3 promoter in CD4<sup>+</sup>CD25<sup>-</sup>Foxp3<sup>-</sup> T cells, and by contrast, a 5-fold decrease of IRF-1 binding in CD4<sup>+</sup>CD25<sup>+</sup>Foxp3<sup>high</sup> human Treg cells (Fig. 6C). Similarly, the binding of IRF-1 to the Foxp3 promoter in the mouse Treg cells was decreased by  $\sim 50\%$  (Fig. 6D).

Finally, to assess the functionality of the in vivo IRF-1 binding, negatively selected primary human and mouse CD4<sup>+</sup> T lymphocytes were nucleofected with the Foxp3 luciferase reporter gene along with expression vector for IRF-1. Fig. 6E shows the results obtained with T cells from three different healthy donors and Fig. 6F shows a representative experiment with mouse T cells from three independent experiments. In all samples, a discrete basal activity of *foxp3* gene promoter was present and this activity was significantly repressed by IRF-1.

## Discussion

The identification of molecules controlling Treg differentiation and function is important not only in understanding host immune responses in malignancy and autoimmunity but also in shaping immune response.

In this study, we have shown that IRF-1, a transcription factor involved in the IFN signaling, selectively affects CD4<sup>+</sup>CD25<sup>+</sup> Treg cell development and function, unraveling a novel immunoregulatory function of IRF-1 in addition to its well-established role in balancing Th1 vs Th2 type immune responses. Several lines of evidence support this conclusion: 1) IRF-1<sup>-/-</sup> mice show a selective and marked increase in all lymphoid organs of CD4<sup>+</sup>CD25<sup>+</sup>Foxp3<sup>+</sup> Treg cells; 2) CD4<sup>+</sup>CD25<sup>+</sup> from IRF-1<sup>-/-</sup> mice are characterized by a highly activated and differentiated CD44<sup>high</sup>CD45RB<sup>low</sup>CD62L<sup>low</sup>CTLA-4<sup>high</sup> phenotype and higher levels of Foxp3 that make them to be functionally more suppressive than WT Treg cells; 3) after TGF- $\beta$  treatment, and importantly also in its absence, CD4<sup>+</sup>CD25<sup>-</sup> T cells from KO mice promptly converted into CD4<sup>+</sup>CD25<sup>+</sup>Foxp3<sup>+</sup> Treg with a higher suppressive activity than WT cells; 4) forced retrovirus-mediated expression of IRF-1 in IRF-1<sup>-/-</sup> CD4<sup>+</sup>CD25<sup>-</sup> T cells impairs their differentiation into CD25<sup>+</sup>Foxp3<sup>+</sup> cells; and 5) IRF-1 directly regulates transcriptional activity of the *foxp3* gene promoter.

The phenotypical and functional characteristics of IRF-1<sup>-/-</sup> Treg cells strongly support the conclusion that IRF-1 can be considered a key negative regulator of CD4<sup>+</sup>CD25<sup>+</sup> Treg cells.

Taken together, the increased frequency of differentiated and activated CD4<sup>+</sup>CD25<sup>+</sup> Treg cells characterized by an immunosuppressive cytokine profile described in this study may provide a mechanistic base for the reduced incidence and severity of several autoimmune diseases characterizing IRF-1<sup>-/-</sup> mice (29–32). In this regard, it has been recently shown that CD4<sup>+</sup>CD25<sup>+</sup> Treg cells were increased in IRF-1<sup>-/-</sup> mice backcrossed with the MRL/lpr mice, which showed reduced glomerulonephritis (44).

The increased production of the immunosuppressive cytokine IL-10 by isolated Treg cells from IRF-1<sup>-/-</sup> mice and the reverted suppression ability of iTreg by anti-IL-10 Abs suggest that this cytokine could play a key role in their suppressor function. Consistently, IL-10 activity has been recently associated with the function of TGF- $\beta$ -induced CD4<sup>+</sup>CD25<sup>-</sup>CD45RB<sup>low</sup> cells because their suppressive activity was abrogated with anti-IL-10R Ab treatment (13). Moreover, several reports focused on the in vivo IL-10

role in peripheral CD4<sup>+</sup>CD25<sup>+</sup> Treg cell function in various autoimmunity models (10–12), although IL-10 seems not required for the functions of thymically derived Treg cells (1). In contrast with the increased IL-10 production, T cells from IRF-1<sup>-/-</sup> mice failed to produce significant amounts of proinflammatory cytokines such as IFN- $\gamma$  or TNF- $\alpha$ . Accordingly, an inverse relationship between in vivo IFN- $\gamma$  administration and generation or activation of CD4<sup>+</sup>CD25<sup>+</sup> Treg cells has been recently shown (45). Moreover, in humans, it has been reported that TNF- $\alpha$  inhibits the suppressive function of both naturally occurring CD4<sup>+</sup>CD25<sup>+</sup> Treg and TGF- $\beta$ -induced Treg cells, and an anti-TNF Ab therapy reversed their suppressive activity by down-modulating the expression of Foxp3 (46). These latter and our results are apparently in contrast with what was recently reported on the stimulating role of IFN- $\gamma$  on Foxp3 induction and conversion of CD4<sup>+</sup>CD25<sup>-</sup> T cells to CD4<sup>+</sup> Treg cells in the IFN- $\gamma$  KO model (47). In this regard, it is noteworthy to underline that, as it has been also suggested, although knocking down genes involved in up-regulation of IFN- $\gamma$  expression do not significantly influence autoimmunity, by contrast the absence of genes expressed in response to IFN- $\gamma$ , including IRF-1, lead to greatly reduced autoimmunity (48). Thus, although the exact mechanism underlying IFN- $\gamma$  and TNF- $\alpha$  interference with the elicitation of Treg cells remains to be defined, we can speculate that induction of IRF-1 expression, which is up-regulated by IFN- $\gamma$  and TNF- $\alpha$ , may represent a mechanism through which proinflammatory cytokines negatively affect Foxp3 expression, thereby influencing generation or activation of CD4<sup>+</sup>CD25<sup>+</sup> Treg cells.

It is well known that Foxp3 plays a pivotal role in the regulatory functions of CD4<sup>+</sup>CD25<sup>+</sup> T cells both in humans and in animal models (5–7). Thus, the key question in the field of Treg biology is which are molecules and signals that govern Foxp3 transcription. In our study, we identify Foxp3 as specific target of IRF-1 and we show that it binds to *foxp3* gene promoter in vitro and in vivo and represses its expression. Recently, structure of the human *foxp3* gene promoter and elements necessary for its induction in T cells have been reported (38). We have identified an IRF-E sequence at 203 bp upstream of the transcriptional start site that is highly conserved. This element is bound by IRF-1 as proven by pull-down experiments and by ChIP analysis in intact cells, and IRF-1 binding resulted in a specific, dose-dependent repression of the *foxp3* proximal promoter. Notably, treatments with IFN- $\gamma$ , a major IRF-1 inducer, significantly inhibited *foxp3* gene promoter transcriptional activity, whereas IRF-2 did not have any effects. Although several features of mouse and human Treg cells appear different (1–3), it is noteworthy that the *foxp3* gene is highly conserved between these species (38), and in particular, the core promoter and the IRF-E identified in this study are perfectly conserved between mouse and human. Such conservation underscores the importance of this motif as regulatory element and provides additional evidence for the role of IRF-1 in regulating *foxp3* gene expression. Accordingly we have shown that IRF-1 binds this sequence and negatively regulates its expression in both human and mouse cells. The molecular interactions enabling IRF-1 to inhibit Foxp3 are not yet identified, although our preliminary results show that IRF-1 may compete with c-Myb for the binding to the same overlapping consensus sequence on the *foxp3* gene promoter.

IRF-1 has a highly complex role in Th cell differentiation by directly affecting the expression of specific genes (27). In this respect, both p35 and p40 subunits of *il12* gene are direct targets of IRF-1-positive transcriptional activity as well as the IL-12R  $\beta$ 1 subunit that is essential for IFN- $\gamma$ -IL-12 signaling (49). Of consequence, the Th2 response-prone phenotype of IRF-1<sup>-/-</sup> mice results from a lack of IL-12 production by macrophages (23, 24) and

DC (33). In contrast, IRF-1 binds three different sites in the *il4* promoter and represses *il4* transcription (42). The overall effect is a vigorous promotion of a Th1 response and an inhibition toward Th2 differentiation pathway, so that IRF-1 has been defined as a “super” Th1 transcription factor (27). The differentiation of naive CD4<sup>+</sup> T cells into Th1 and Th2 cells is supplemented by a TGF- $\beta$ -driven pathway for the differentiation of iTreg cells that develop from naive T cells in absence of IL-4 and IL-12. TGF- $\beta$  facilitates this pathway by inhibiting IL-4 and IL-12 and the transcription factors GATA-3 and T-bet, and by inducing Foxp3 (50). In this context, it has been recently reported that GATA-3 inhibits Foxp3 expression and formation of Treg cells by binding to the *foxp3* proximal promoter and suppressing its transcriptional activity (51). Therefore GATA-3 not only induces Th2 differentiation but also inhibits commitment into Treg cells (51). In a similar fashion, the current study reveals that IRF-1, which is a key regulator for polarization toward Th1 cells, directly represses Foxp3 expression and Treg cell development.

In summary, the current study provides evidence that IRF-1 affects CD4<sup>+</sup>CD25<sup>+</sup> development and function by Foxp3 repression. Thus, our data demonstrate a new important contribution by which IRF-1 affects T cell differentiation and provide new important insights into molecular mechanisms controlling immune homeostasis.

## Acknowledgments

We thank Dr. Yutaka Tagaya for providing IRF-1<sup>-/-</sup> mice, Dr. M. Li-Weber, Dr. K. L. Wright, and Dr. K. Ozato for providing luciferase constructs and expression vectors, and Dr. S. Vendetti for helpful critical reading of the manuscript. We thank R. Gilardi for artwork.

## Disclosures

The authors have no financial conflict of interest.

## References

- Sakaguchi, S. 2004. Naturally arising CD4<sup>+</sup> regulatory T cells for immunologic self-tolerance and negative control of immune responses. *Annu. Rev. Immunol.* 22: 531–562.
- Schevach, E. M. 2006. From vanilla to 28 flavours: multiple varieties of T regulatory cells. *Immunity* 25: 195–201.
- Campbell, D. J., and S. F. Ziegler. 2007. FoxP3 modifies the phenotypic and functional properties of regulatory T cells. *Nat. Rev. Immunol.* 7: 305–310.
- Yi, H., Y. Zhen, L. Jiang, J. Zheng, and Y. Zhao. 2006. The phenotypic characterization of naturally occurring regulatory CD4<sup>+</sup>CD25<sup>+</sup> T cells. *Cell. Mol. Immunol.* 3: 189–195.
- Fontenot, J. D., M. A. Gavin, and A. Y. Rudensky. 2003. Foxp3 programs the development and function of CD4<sup>+</sup>CD25<sup>+</sup> regulatory T cells. *Nat. Immunol.* 4: 330–336.
- Hori, S., T. Nomura, and S. Sakaguchi. 2003. Control of regulatory T cell development by the transcription factor Foxp3. *Science* 299: 1057–1061.
- Khattry, R., T. S. Cox, A. Yasayko, and F. Ramsdell. 2003. An essential role for Scurfin in CD4<sup>+</sup>CD25<sup>+</sup> T regulatory cells. *Nat. Immunol.* 4: 337–342.
- Thornton, A. M., and E. M. Shevach. 1998. CD4<sup>+</sup>CD25<sup>+</sup> immunoregulatory T cells suppress polyclonal T cell activation in vitro by inhibiting interleukin 2 production. *J. Exp. Med.* 188: 287–296.
- Maloy, K. J., L. Salaun, R. Cahill, G. Dougan, N. J. Saunders, and F. Powrie. 2003. CD4<sup>+</sup>CD25<sup>+</sup> T<sub>R</sub> cells suppress innate immune pathology through cytokine-dependent mechanisms. *J. Exp. Med.* 197: 111–119.
- Suri-Payer, E., and H. Cantor. 2001. Differential cytokine requirements for regulation of autoimmune gastritis and colitis by CD4<sup>+</sup>CD25<sup>+</sup> T cells. *J. Autoimmun.* 16: 115–123.
- Liu, H., B. Hu, D. Xu, and F. Y. Liew. 2003. CD4<sup>+</sup>CD25<sup>+</sup> regulatory T cells cure murine colitis the role of IL-10, TGF- $\beta$  and CTLA4. *J. Immunol.* 171: 5012–5017.
- Annacker, O., R. Pimenta-Araujo, O. T. Burlen-Defranoux, T. C. Barbosa, A. Cumano, and A. Bandeira. 2001. CD25<sup>+</sup>CD4<sup>+</sup> T cells regulate the expansion of peripheral CD4 T cells through the production of IL-10. *J. Immunol.* 166: 3008–3018.
- Pyzik, M., and C. A. Piccirillo. 2007. TGF- $\beta$ 1 modulates Foxp3 expression and regulatory activity in distinct CD4<sup>+</sup> T cell subsets. *J. Leukocyte Biol.* 82: 335–346.
- Chen, W., W. Jin, N. Hardegen, K. J. Lei, L. Li, N. Marinos, G. McGrady, and S. M. Wahl. 2003. Conversion of peripheral CD4<sup>+</sup>. *J. Exp. Med.* 198: 1875–1886.

15. Zheng, S. G., J. H. Wang, W. Stohl, K. S. Kim, J. D. Gray, and D. A. Horwitz. 2006. TGF- $\beta$  requires CTLA-4 early after T cell activation to induce Foxp3 and generate adaptive CD4<sup>+</sup>CD25<sup>+</sup> regulatory cells. *J. Immunol.* 176: 3321–3329.
16. Liang, S., P. Alard, Y. Zhao, S. Pamell, S. L. Clark, and M. M. Kosiewicz. 2005. Conversion of CD4<sup>+</sup>. *J. Exp. Med.* 201: 127–137.
17. Fantini, M. C., C. Becker, G. Monteleone, F. Pallone, P. R. Galle, and M. F. Neurath. 2004. Cutting edge: TGF- $\beta$  induces a regulatory phenotype in CD4<sup>+</sup>. *J. Immunol.* 172: 5149–5153.
18. Walker, M. R., D. J. Kasprowitz, V. H. Gersuk, A. Benard, L. M. Van, J. H. Buckner, and S. F. Ziegler. 2003. Induction of FoxP3 and acquisition of T regulatory activity by stimulated human CD4<sup>+</sup>. *J. Clin. Invest.* 112: 1437–1443.
19. Wan, Y. Y., and R. A. Flavell. 2005. Identifying Foxp3-expressing suppressor T cells with a bicistronic reporter. *Proc. Natl. Acad. Sci. USA* 102: 5126–5131.
20. Tran, D. Q., H. Ramsey, and E. M. Shevach. 2007. Induction of FOXP3 expression in naive human CD4<sup>+</sup>FOXP3<sup>-</sup> T cells by T cell receptor stimulation is TGF $\beta$ -dependent but does not confer a regulatory phenotype. *Blood* 110: 2983–2990.
21. Taniguchi, T., K. Ogasawara, A. Takaoka, and N. Tanaka. 2001. IRF family of transcription factors as regulators of host defense. *Annu. Rev. Immunol.* 19: 623–655.
22. Miyamoto, M., T. Fujita, Y. Kimura, M. Maruyama, H. Harada, Y. Sudo, T. Miyata, and T. Taniguchi. 1988. Regulated expression of a gene encoding a nuclear factor, IRF-1, that specifically binds to IFN- $\beta$  gene regulatory elements. *Cell* 54: 903–913.
23. Matsuyama, T., T. Kimura, M. Kitagawa, K. Pfeffer, T. Kawakami, N. Watanabe, T. M. Kundig, R. Amakawa, K. Kishihara, A. Wakeham, and T. K. Taniguchi. 1993. Targeted disruption of IRF-1 or IRF-2 results in abnormal type I IFN gene induction and aberrant lymphocyte development. *Cell* 75: 83–97.
24. Lohoff, M., D. Ferrick, H. W. Mittrucker, G. S. Duncan, S. Bischof, M. Rollinghoff, and T. W. Mak. 1997. Interferon regulatory factor-1 is required for a T helper 1 immune response in vivo. *Immunity* 6: 681–689.
25. Ogasawara, K., S. Hida, N. Azimi, Y. Tagaya, T. Sato, T. Yokochi-Fukuda, T. A. Waldmann, T. Taniguchi, and S. Taki. 1998. Requirement for IRF-1 in the microenvironment supporting development of natural killer cells. *Nature* 391: 700–703.
26. Testa, U., E. Stellacci, E. Pelosi, P. Sestili, M. Venditti, R. Orsatti, A. Fragale, E. Petrucci, L. Pasquini, F. Belardelli, L. Gabriele, and A. Battistini. 2004. Impaired myelopoiesis in mice devoid of interferon regulatory factor 1. *Leukemia* 18: 1864–1871.
27. Lohoff, M., and T. W. Mak. 2005. Roles of interferon-regulatory factors in T-helper-cell differentiation. *Nat. Rev. Immunol.* 5: 125–135.
28. Coccia, E. M., E. Stellacci, M. Valtieri, B. Masella, T. Feccia, G. Marziali, J. Hiscott, U. Testa, C. Peschle, and A. Battistini. 2001. Ectopic expression of interferon regulatory factor-1 potentiates granulocytic differentiation. *Biochem. J.* 360: 285–294.
29. Tada, Y., A. Ho, T. Matsuyama, and T. W. Mak. 1997. Reduced incidence and severity of antigen-induced autoimmune diseases in mice lacking interferon regulatory factor-1. *J. Exp. Med.* 185: 231–238.
30. Buch, T., C. Uthoff-Hachenberg, and A. Waisman. 2003. Protection from autoimmune brain inflammation in mice lacking IFN-regulatory factor-1 is associated with Th2-type cytokines. *Int. Immunol.* 15: 855–859.
31. Sommer, F., G. Faller, M. Röllinghoff, T. Kirchner, T. W. Mak, and M. Lohoff. 2001. Lack of gastritis and of an adaptive immune response in interferon regulatory factor-1-deficient mice infected with *Helicobacter pylori*. *Eur. J. Immunol.* 31: 396–402.
32. Nakazawa, T., J. Satoh, K. Takahashi, Y. Sakata, F. Ikehata, Y. Takizawa, S. I. Bando, T. Housai, Y. Li, C. Chen, et al. 2001. Complete suppression of insulinitis and diabetes in NOD mice lacking interferon regulatory factor-1. *J. Autoimmun.* 17: 119–125.
33. Gabriele, L., A. Fragale, P. Borghi, P. Sestili, E. Stellacci, M. Venditti, G. Schiavoni, M. Sanchez, F. Belardelli, and A. Battistini. 2006. IRF-1 deficiency skews the differentiation of dendritic cells toward plasmacytoid and tolerogenic features. *J. Leukocyte Biol.* 80: 1500–1511.
34. Steinman, R. M., D. Hawiger, and M. C. Nussenzweig. 2003. Tolerogenic dendritic cells. *Annu. Rev. Immunol.* 21: 685–711.
35. Tarbell, K. V., S. Yamazaki, and R. M. Steinman. 2006. The interactions of dendritic cells with antigen-specific, regulatory T cells that suppress autoimmunity. *Semin. Immunol.* 18: 93–102.
36. Dror, N., M. ter-Koltunoff, A. Azriel, N. Amariglio, J. Jacob-Hirsch, S. Zeligson, A. Morgenstern, T. Tamura, H. Hauser, G. Rechavi, et al. 2007. Identification of IRF-8 and IRF-1 target genes in activated macrophages. *Mol. Immunol.* 44: 338–346.
37. Pop, S. M., C. P. Wong, D. A. Culton, S. H. Clarke, and R. Tisch. 2005. Single cell analysis shows decreasing FoxP3 and TGF $\beta$ 1 coexpressing CD4<sup>+</sup>CD25<sup>+</sup> regulatory T cells during autoimmune diabetes. *J. Exp. Med.* 201: 1333–1346.
38. Mantel, P. Y., N. Ouaked, B. Ruckert, C. Karagiannidis, R. Welz, K. Blaser, and C. B. Schmidt-Weber. 2006. Molecular mechanisms underlying FoxP3 induction in human T cells. *J. Immunol.* 176: 3593–3602.
39. Sgarbanti, M., A. Borsetti, N. Moscufo, M. C. Bellocchi, B. Ridolfi, F. Nappi, G. Marsili, G. Marziali, E. M. Coccia, B. Ensoli, and A. Battistini. 2002. Modulation of human immunodeficiency virus 1 replication by interferon regulatory factors. *J. Exp. Med.* 195: 1359–1370.
40. Remoli, A. L., G. Marsili, E. Perrotti, E. Gallerani, R. Ilari, F. Nappi, A. Cafaro, B. Ensoli, R. Gavioli, and A. Battistini. 2006. Intracellular HIV-1 Tat protein represses constitutive LMP2 transcription increasing proteasome activity by interfering with the binding of IRF-1 to STAT1. *Biochem. J.* 396: 371–380.
41. McElligott, D. L., J. A. Phillips, C. A. Stillman, R. J. Koch, D. E. Mosier, and M. V. Hobbs. 1997. CD4<sup>+</sup> T cells from IRF-1-deficient mice exhibit altered patterns of cytokine expression and cell subset homeostasis. *J. Immunol.* 159: 4180–4186.
42. Elser, B., M. Lohoff, S. Kock, M. Giaisi, S. Kirchhoff, P. H. Krammer, and M. Li-Weber. 2002. IFN- $\gamma$  represses IL-4 expression via IRF-1 and IRF-2. *Immunity* 17: 703–712.
43. White, L. C., K. L. Wright, N. J. Felix, H. Ruffner, L. F. Reis, R. Pine, and J. P. Ting. 1996. Regulation of LMP2 and TAP1 genes by IRF-1 explains the paucity of CD8<sup>+</sup> T cells in IRF-1<sup>-/-</sup> mice. *Immunity* 5: 365–376.
44. Reilly, C. M., S. Olgun, D. Goodwin, R. M. Gogal, Jr., A. Santo, J. W. Romesburg, S. A. Ahmed, and G. S. Gilkeson. 2006. Interferon regulatory factor-1 gene deletion decreases glomerulonephritis in MRL/lpr mice. *Eur. J. Immunol.* 36: 1296–1308.
45. Nishikawa, H., T. Kato, I. Tawara, H. Ikeda, K. Kuribayashi, P. M. Allen, R. D. Schreiber, L. J. Old, and H. Shiku. 2005. IFN- $\gamma$  controls the generation/activation of CD4<sup>+</sup>CD25<sup>+</sup> regulatory T cells in antitumor immune response. *J. Immunol.* 175: 4433–4440.
46. Valencia, X., G. Stephens, R. Goldbach-Mansky, M. Wilson, E. M. Shevach, and P. E. Lipsky. 2006. TNF down-modulates the function of human CD4<sup>+</sup>CD25<sup>hi</sup> T regulatory cells. *Blood* 108: 253–261.
47. Wang, Z., J. Hong, W. Sun, G. Xu, N. Li, X. Chen, A. Liu, L. Xu, B. Sun, and J. Z. Zhang. 2006. Role of IFN- $\gamma$  in induction of Foxp3 and conversion of CD4<sup>+</sup>. *J. Clin. Invest.* 116: 2434–2441.
48. Pollard, K. M., P. Hultman, and D. H. Kono. 2005. Immunology and genetics of induced systemic autoimmunity. *Autoimmun. Rev.* 4: 282–288.
49. Kano, S., K. Sato, Y. Morishita, S. Vollstedt, S. Kim, K. Bishop, K. Honda, M. Kubo, and T. Taniguchi. 2008. The contribution of transcription factor IRF1 to the interferon- $\gamma$ -interleukin 12 signaling axis and T<sub>H</sub>1 versus T<sub>H</sub>17 differentiation of CD4<sup>+</sup> T cells. *Nat. Immunol.* 9: 34–41.
50. Wahl, S. M., N. Vazquez, and W. Chen. 2004. Regulatory T cells and transcription factors: gatekeepers in allergic inflammation. *Curr. Opin. Immunol.* 16: 768–774.
51. Mantell P.-Y., H. Kuipers, O. Boyma, C. Rhyner, N. Ouaked, B. Ruchert, C. Karagiannidis, B. N. Lambrecht, R. W. Hendriks, R. Cramer, et al. 2008. GATA3-driven Th2 response inhibit TGF- $\beta$ 1-induced FOXP3 expression and the formation of regulatory T cells. *PLOS Biol.* 5: 2847–2861.